Supplementary information

Supplementary information, Data S1

Materials and Methods

Animal information

All the experimental procedures were performed in compliance with the protocols approved by the Institutional Animal Care and Use Committee (IACUC) of Peking University. The mice utilized in the experiments were 8-12 weeks old. C57BL/6 wild-type mice were purchased from Charles River International. *Cx3cr1*$^{EYFP/EYFP}$ (JAX 021160, RRID:IMSR_JAX:021160), *Th-Cre* (JAX 008601, RRID:IMSR_JAX:008601), *TrkA*$^{fl/fl}$ (JAX 022362, RRID:IMSR_JAX:022362) and *Sarm1*$^{-/-}$ (JAX 018069, RRID:IMSR_JAX:018069) were purchased and bred in-house to generate the littermates for experiments.

For the chemotherapy-induced neuropathy, Paclitaxel (Sigma) was formulated in DMSO/Kolliphor-EL/0.9% saline (v:v:v = 5:20:75) to the final concentration of 5 mg/mL. The mice were administered daily at 20 mg/kg of body weight via intravenous injection for 6 days. For the control condition, the mice were administered daily with the vehicle solution.

For the sciatic nerve injury, the skin on the left hindlimb of anesthetized mice was shaved and sterilized with iodine and alcohol. The skin incision was made between the knee and the hip joint, and the gluteal muscles were separated to expose the sciatic nerve. The nerve was crushed with a pair of sterile forceps for 20 s. The gluteal muscles were

then brought back into their original anatomical position, and the skin incision was closed by surgical staples.

BoneClear procedure

This procedure has been optimized for the whole-tissue immunolabeling of the intact, unsectioned mouse bone tissues, e.g., femur, vertebral column, skull, and hindpaw. The anesthetized mice were perfused with 25 mL PBS/50 μg/mL heparin, followed by 25 mL PBS/1% PFA/10% sucrose/50 μg/mL heparin. The tissues were dissected out, and post-fixed in PBS/0.5% PFA/10% sucrose at room temperature for 2 h. The tissues were further fixed in PBS/0.5% PFA at 4 °C overnight and then washed with PBS at room temperature for 1 h three times. The tissues were decalcified in 350 mM EDTA-Na (pH 6.5) at 37 °C for 72 h, with the fresh buffer changed every 24 h. All the incubation steps were performed with gentle shaking.

The decalcified tissues were incubated at room temperature with the methanol gradient (diluted in ddH_2O): 20% methanol for 2 h, 40% methanol for 2 h, 60% methanol for 2 h, 80% methanol for 2 h, and 100% methanol for 2 h twice. The tissues were decolorized at 4 °C overnight with the mixture of 30% H_2O_2 and 100% methanol (v:v = 1:10). The tissues were incubated at room temperature with the inverse methanol gradient (diluted in ddH_2O): 100% methanol for 2 h, 80% methanol for 2 h, 60% methanol for 2 h, 40% methanol for 2 h, 20% methanol for 2 h, and PBS for 2 h. The tissues were permeabilized with PBS/0.2% Triton X-100/0.1% Deoxycholate/10% DMSO/25 mM EDTA (pH 6.5) at 37 °C overnight, and then blocked with PBS/0.2% Triton X-100/10%

DMSO/5% normal donkey serum/25 mM EDTA (pH 6.5) at 37 °C overnight. All the incubation steps were performed with gentle shaking.

The tissues were immunolabeled with the primary antibodies diluted (1:500) in PBS/0.2% Tween-20/10 μg/mL heparin/5% normal donkey serum/25 mM EDTA (pH 6.5) at 37 °C for 72 h. The primary antibodies used in this study: rabbit anti-PGP9.5 (Proteintech Group, Cat#14730-1-AP, RRID:AB_2210497), rabbit anti-Tyrosine Hydroxylase (Millipore, Cat#AB152, RRID:AB_390204), chicken anti-EGFP (Aves Labs, Cat#GFP-1010, RRID:AB_2307313), rat anti-PECAM1 (BD Biosciences, Cat#553370, RRID:AB_394816), rabbit anti-SOX9 (Millipore, Cat#AB5535, RRID:AB_2239761), rabbit anti-Glial Fibrillary Acidic Protein (Millipore, Cat#AB5804, RRID:AB_2109645), chicken anti-Tyrosine Hydroxylase (Millipore, Cat#AB9702, RRID:AB_570923), goat anti-VEGFR3 (R&D Systems, Cat#AF743, RRID:AB_355563), and rabbit anti-Synaptophysin (Thermo Fisher Scientific, Cat#180130, RRID:AB_10836766). The tissues were washed with PBS/0.2% Tween-20/10 μg/mL heparin/25 mM EDTA (pH 6.5) at 37 °C for 24 h, with the fresh buffer changed every 6 h. The tissues were further immunolabeled with the Alexa Fluor-conjugated secondary antibodies (Thermo Fisher Scientific) diluted (1:500) in PBS/0.2% Tween-20/10 μg/mL heparin/5% normal donkey serum/25 mM EDTA (pH 6.5) at 37 °C for 72 h. Of note, incubation with the primary or secondary antibodies at 37 °C for 72 h is sufficient for the whole-tissue immunolabeling of the mouse bone tissues examined in the current study. However, for other tissues and/or certain antibodies, a longer time of incubation may be necessary and needs to be determined experimentally. The tissues were washed with PBS/0.2% Tween-20/10 μg/mL heparin/25 mM EDTA (pH 6.5) at 37 °C for 48 h, with

the fresh buffer changed every 6 h. All the incubation steps were performed with gentle shaking.

The optical-clearing steps for the immunolabeled tissues have been optimized based on the iDISCO+ method. The tissues were embedded in PBS/0.8% agarose. The tissue blocks were incubated at room temperature with the methanol gradient (diluted in ddH_2O): 20% methanol for 4 h, 40% methanol for 2 h, 60% methanol for 2 h, 80% methanol for 2 h, and 100% methanol for 2 h twice. The tissue blocks were then incubated at room temperature with the mixture of dichloromethane and methanol (v:v = 2:1) for 2 h twice, followed by 100% dichloromethane for 30 min four times. The tissue blocks were cleared at room temperature with 100% dibenzyl-ether for 12 h three times. All the incubation steps were performed with gentle shaking.

3D Fluorescence imaging

For the lightsheet microscope, the optically-cleared tissues were imaged on the LaVision Biotec Ultramicroscope II equipped with the sCMOS camera (Andor Neo) and the 2×/NA 0.5 objective (MVPLAPO) covered with the 6 mm-working-distance dipping-cap. Version 144 of the ImSpector Microscope Controller software was supported by LaVision Biotec. The tissues were immersed in the imaging chamber filled with 100% dibenzyl-ether. For imaging at 1.26× magnification, each tissue was scanned by three combined lightsheets from the left side with a step size of 4 μm. For imaging at 12.6× magnification, each tissue was scanned by a single lightsheet (middle position) from the left side with a step size of 1 μm. The image stacks were acquired by the continuous lightsheet scanning method without the contrast-blending algorithm.

For the confocal microscope, the optically-cleared tissues were imaged on the Nikon A1R MP+ Confocal Microscope equipped with the 20×/NA 0.75 Plan Apo objective. Each tissue was placed between two coverslips and imaged with a step size of 1.1 μm.

Imaris (https://imaris.oxinst.com/packages) was used to reconstruct the image stacks. For the display purpose in the figures and movies, a gamma correction of 1.3-1.6 was applied to the raw data. Orthogonal 3D projections of the image stacks were generated for the representative images shown in the figures. The movies were produced with a frame rate of 30 fps.

Statistical method

To quantify the spatial engagement of the neural innervations with the vasculatures in the femurs, three 400 μm × 400 μm × 400 μm cubic volumes were randomly selected along the middle shaft from the reconstructed 3D images of each femur. The percentage of the PGP9.5-positive axons that resided < 10 μm from the PECAM1-positive vasculatures was manually examined in each cubic volume. To quantify the spatial engagement of the glial cells with the sympathetic axons or the vasculatures, three 400 μm × 400 μm × 400 μm cubic volumes were randomly selected along the middle shaft from the reconstructed 3D images of each femur. The percentage of the GFAP-positive glial cells that resided < 10 μm from the TH-positive sympathetic axons or the PECAM1-positive vasculatures were manually examined in each cubic volume.

To quantify the sympathetic innervations in the femurs, three 400 μm × 400 μm × 400 μm cubic volumes were randomly selected along the middle shaft from the reconstructed 3D images of each femur. The length of the TH-positive axons in each cubic volume was manually traced. To quantify the neural innervations in the hindpaws, three 200 μm × 200 μm × 200 μm cubic volumes were randomly selected from the reconstructed 3D images of the nail, digit tip or skin. The length of the PGP9.5-positive axons in each cubic volume was manually traced.

Student's two-sided *t*-test or ANOVA test was performed using GraphPad Prism (http://www.graphpad.com/scientific-software/prism). Statistical details of the experiments are included in the figure legends.

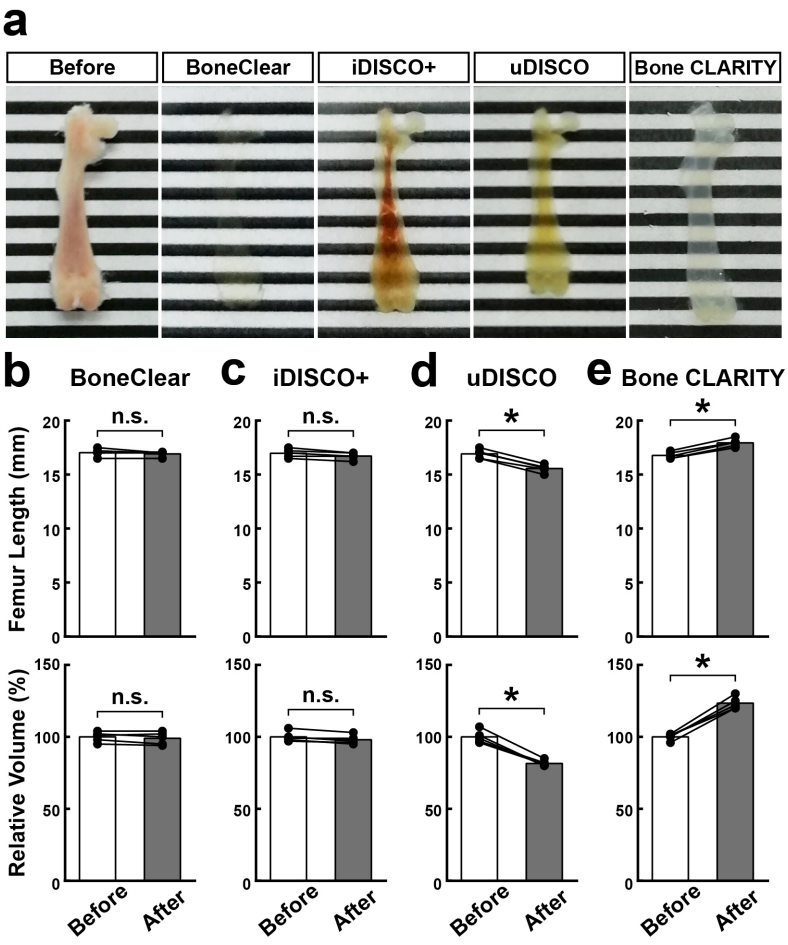

Supplementary information, Fig. S1 Comparison of BoneClear with the published methods for optical clearing of the mouse femurs. a The intact, unsectioned femurs of adult mice before (left panel) and after the procedure of BoneClear, iDISCO+, uDISCO or Bone CLARITY (right panels). **b-e** Length (upper panels) and tissue volume (lower panels) of the femurs before and after the procedure of BoneClear **(b)**, iDISCO+ **(c)**, uDISCO **(d)** or Bone CLARITY **(e)** were measured. n = 5, n.s., not significant; * $p < 0.01$ (Student's *t*-test).

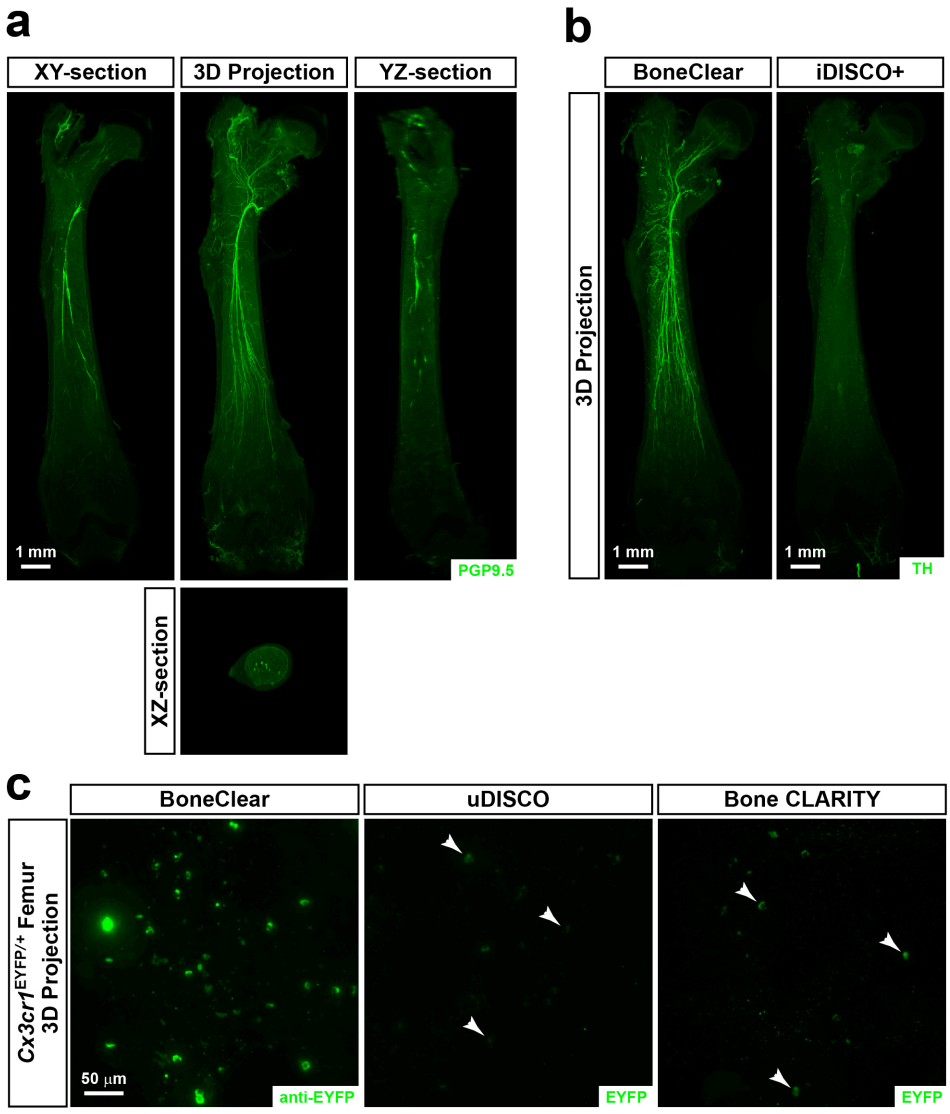

Supplementary information, Fig. S2 Comparison of BoneClear with the published methods for whole-tissue immunolabeling and 3D imaging of the mouse femurs.

a The intact, unsectioned mouse femur was processed for the whole-tissue PGP9.5-immunolabeling by BoneClear. Representative 3D-projection image at 1.26x magnification on the lightsheet microscope (upper-middle panel), and representative XY-section (upper-left panel), YZ-section (upper-right panel) and XZ-section (lower panel) of the image stack were shown. **b** The femurs were processed for the whole-tissue TH-

immunolabeling by BoneClear (left panel) or iDISCO+ (right panel). Representative 3D-projection images at 1.26x magnification on the lightsheet microscope were shown. **c** The femurs of *Cx3cr1*$^{EYFP/+}$ mice were processed by BoneClear for the whole-tissue EYFP-immunolabeling (left panel), or by uDISCO (middle panel) or Bone CLARITY (right panel) for visualizing the EYFP fluorescence signal. The tissues were imaged at 12.6x magnification on the lightsheet microscope under the same parameters. Representative 3D-projection images of 300 μm-depth bone marrow were shown. Arrowheads denote the EYFP-positive cells revealed by uDISCO or Bone CLARITY.

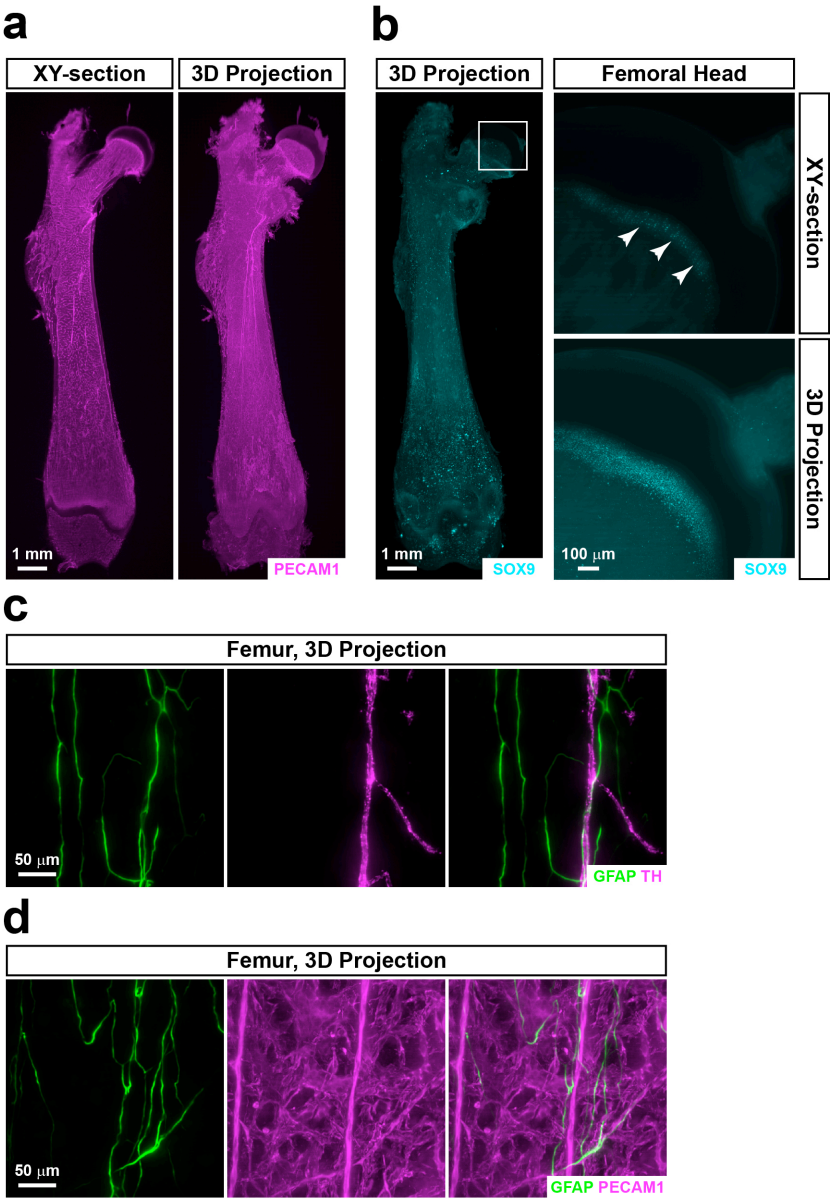

Supplementary information, Fig. S3 Whole-tissue immunolabeling of different cellular structures in the mouse femurs. **a** The intact, unsectioned mouse femur was processed for the whole-tissue PECAM1-immunolabeling to visualize the vasculatures. Representative 3D-projection image at 1.26x magnification on the lightsheet microscope (right panel) and representative XY-section of the image stack (left panel) were shown. **b** The femur was processed for the whole-tissue SOX9-immunolabeling to visualize the

chondrocytes. Representative 3D-projection image at 1.26x magnification on the lightsheet microscope (left panel, the square denotes the region imaged at 12.6x magnification), and representative 3D-projection image (lower-right panel) and XY-section (upper-right panel) of the femoral head at 12.6x magnification were shown. Arrowheads denote the SOX9-positive nuclei of the chondrocytes. **c, d** The femurs were processed for the whole-tissue co-immunolabeling of GFAP and TH **(c)**, or GFAP and PECAM1 **(d)**. Representative 3D-projection images of 300 μm-depth bone marrow at 12.6x magnification on the lightsheet microscope were shown.

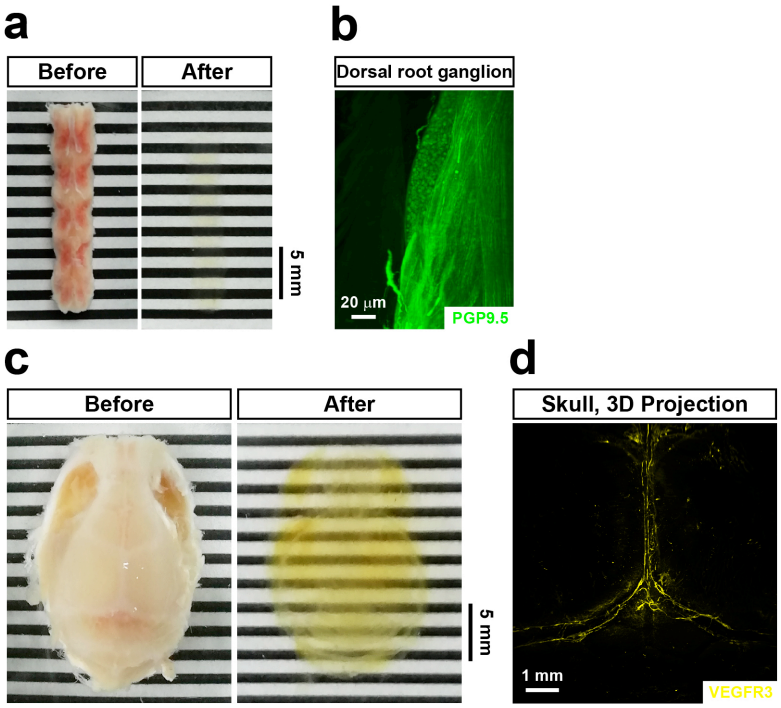

Supplementary information, Fig. S4 Whole-tissue immunolabeling of different cellular structures in the mouse bone tissues. **a** The lumbar portion (L1 to L5) of the mouse vertebral column before (left panel) and after (right panel) BoneClear. **b** The lumbar vertebral column was processed for the whole-tissue PGP9.5-immunolabeling. Representative 3D-projection image of the dorsal root ganglion imaged through the vertebrae at 12.6x magnification on the lightsheet microscope was shown. **c** The intact mouse skull before (left panel) and after (right panel) BoneClear. **d** The skull was processed for the whole-tissue VEGFR3-immunolabeling to visualize the lymphatic vessels. Representative 3D-projection image at 1.26x magnification on the lightsheet microscope was shown.

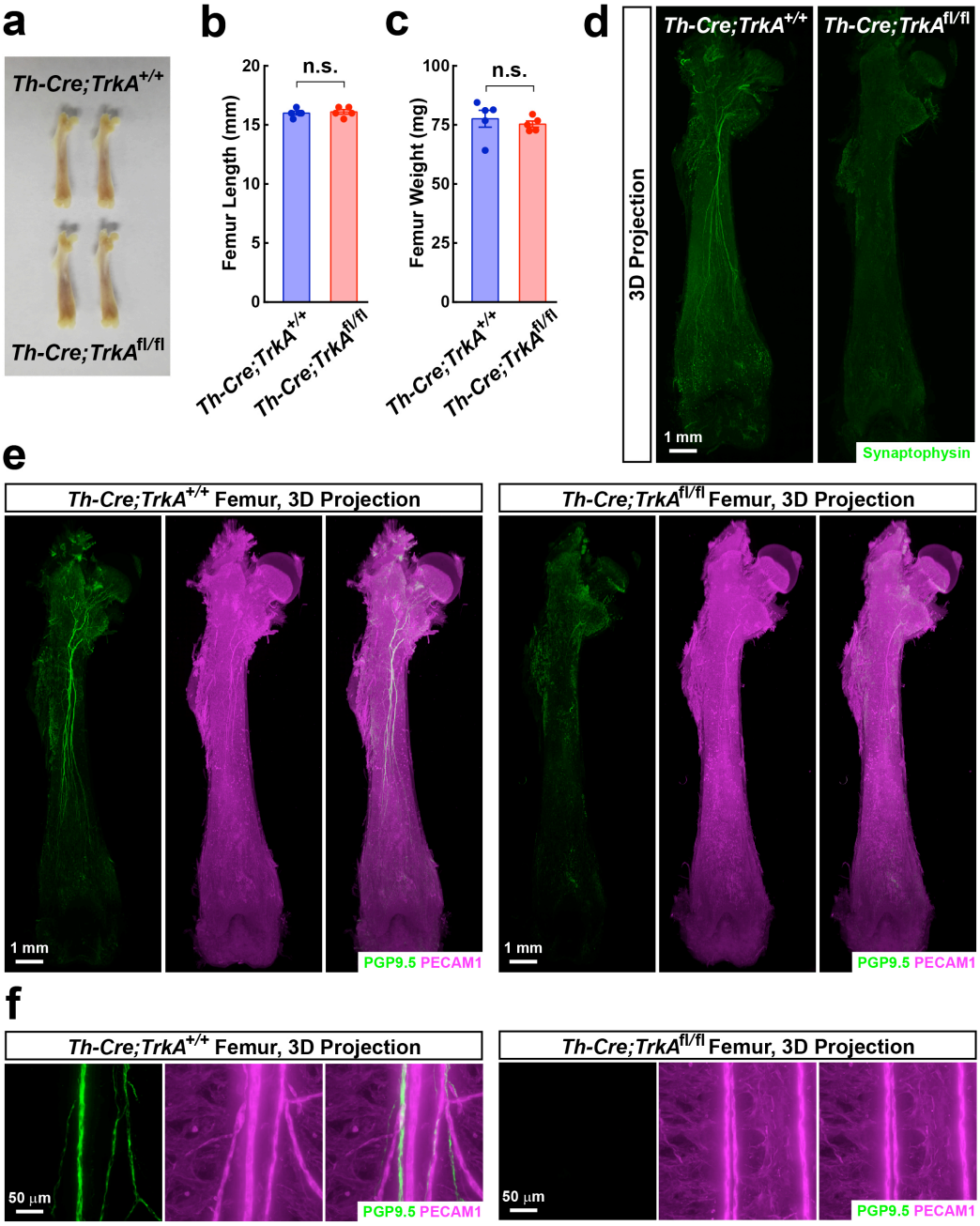

Supplementary information, Fig. S5 Ablation of the intraosseous neural innervations in the femurs of *Th-Cre; TrkA$^{fl/fl}$* mice. a-c Normal development of the femurs of *Th-Cre; TrkA$^{fl/fl}$* mice. Gross appearance of the femurs of *Th-Cre; TrkA$^{+/+}$ vs. Th-Cre; TrkA$^{fl/fl}$* mice **(a)**. Length **(b)** and tissue weight **(c)** of the femurs of *Th-Cre;*

TrkA$^{+/+}$ *vs*. *Th-Cre; TrkA*$^{fl/fl}$ mice were measured. n = 5, mean ± SEM, n.s., not significant (Student's *t*-test). **d-f** Ablation of the intraosseous neural innervations in the *Th-Cre; TrkA*$^{fl/fl}$ femurs. The femurs of *Th-Cre; TrkA*$^{+/+}$ and *Th-Cre; TrkA*$^{fl/fl}$ mice were processed for the whole-tissue immunolabeling of Synaptophysin **(d)** or the co-immunolabeling of PGP9.5 and PECAM1 **(e, f)**. Representative 3D-projection images at 1.26x magnification on the lightsheet microscope **(d, e)**, and representative 3D-projection images of 300 μm-depth bone marrow at 12.6x magnification **(f)** were shown.

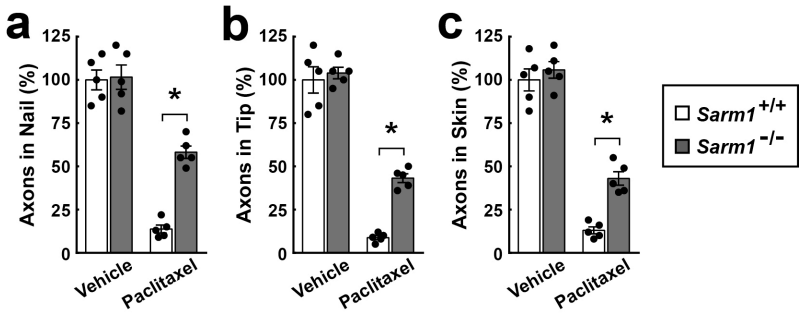

Supplementary information, Fig. S6 Mitigation of the chemotherapy-induced neuropathy in the hindpaws of *Sarm1*$^{-/-}$ mice. a-c *Sarm1*$^{+/+}$ and *Sarm1*$^{-/-}$ mice were treated with Paclitaxel or vehicle control for 6 days. The hindpaws were processed for the whole-tissue PGP9.5-immunolabeling and imaged at 12.6x magnification on the lightsheet microscope. Length of the axons in the nail **(a)**, digit tip **(b)**, and skin **(c)** was quantified. n = 5, mean ± SEM, * $p < 0.01$ (ANOVA test).